Research Article | Vol. 27, No. 23 / 11 November 2019 / Optics Express 33205
Optics EXPRESS

Electrically injected 1.64μm emitting $In_{0.65}Ga_{0.35}As$ 3-QW laser diodes grown on mismatched substrates by MOVPE

H. KIM,[1,*] B. SHI,[2,5] Z. LINGLEY,[3] Q. LI,[2,6] A. RAJEEV,[1] M. BRODIE,[3] K. M. LAU,[3] T. F. KUECH,[4] Y. SIN,[3] AND L. J. MAWST[1]

[1]*Department of Electrical and Computer Engineering, University of Wisconsin-Madison, Madison, Wisconsin 53706, USA*
[2]*Department of Electronic and Computer Engineering, Hong Kong University of Science and Technology, Clear Water Bay, Kowloon, Hong Kong*
[3]*Electronics and Photonics Lab, The Aerospace Corporation, El Segundo, California 90245, USA*
[4]*Department of Chemical and Biological Engineering, University of Wisconsin-Madison, Madison, Wisconsin 53706, USA*
[5]*Now at Department of Electrical and Computer Engineering, University of California, Santa Barbara, California 93106, USA*
[6]*Now at School of Physics and Astronomy, Cardiff University, Cardiff CF10 3AT, UK*
[*]*hkim527@wisc.edu*

Abstract: We report the characteristics of the strained $In_{0.65}Ga_{0.35}As$ triple quantum well (QW) diode lasers grown by metalorganic vapor phase epitaxy (MOVPE) on lattice-mismatched substrates such as GaAs or Si, by utilizing InP metamorphic buffer layers (MBLs) in conjunction with InAs nanostructure-based dislocation filters. As the lattice-mismatch between the substrate and InP MBL increases, higher threshold current densities and lower slope efficiencies were observed, together with higher temperature sensitivities for the threshold current and slope efficiency. Structural analysis performed by both high-resolution X-ray diffraction (HR-XRD) and transmission electron microscopy indicates graded and/or rougher QW interfaces within the active region grown on the mismatched substrate, which accounts for the observed devices characteristics.

1. Introduction

The heteroepitaxy of III-V alloys, lattice-matched to InP, onto mismatched substrates, such as GaAs and Si substrates, have drawn much attention for both electronic and optoelectronic applications. These material combinations take advantage of a lower substrate cost and epitaxial growth on larger available wafer, as well as for the compatibility with the existing high volume Si-based CMOS technology and monolithic integration onto the Si-based optoelectronic platform [1–9]. However, the high defect density, originating from the large mismatch in either lattice constant and/or thermal expansion coefficient [10] between GaAs/InP or Si/InP, has remained as a challenging factor limiting the device performance and reliability [11].

Nevertheless, to date, a number of research groups have demonstrated laser emission near 1.55 μm from a material system grown on mismatched substrates by employing metamorphic buffer layers [4,8–9,12–16]. Furthermore, reliable CW operation from a multiple quantum well (MQW) active region laser was demonstrated when the residual threading dislocation density (TDD) is sufficiently reduced [8].

MBE (Molecular Beam Epitaxy) grown laser structures employing an $In_{0.32}Ga_{0.68}As$ metamorphic buffer layer (MBL) and an $In_{0.6}Ga_{0.4}As$ single quantum well (QW) on GaAs substrate have demonstrated laser emission at 1.58 μm with a low threshold current density (J_{th}) of 0.49 kA/cm^2 [12]. In addition, the MBE growth of a GaSb-based interfacial misfit (IMF) array led to

#374310 https://doi.org/10.1364/OE.27.033205
Journal © 2019 Received 7 Aug 2019; revised 20 Sep 2019; accepted 17 Oct 2019; published 30 Oct 2019

Optics EXPRESS

laser operation at room temperature with emission wavelength of 1.65 μm and J_{th} ~ 3 kA/cm^2 from devices employing a 6-period GaSb/AlGaSb QW active region [13]. The MBE growth of InAs quantum dot (QD) active region lasers on either a GaAsSb [14] or an AlGaAsSb [15] MBLs have demonstrated photoluminescence (PL) emission wavelengths near 1.55 μm although room temperature lasing under pulsed current operation occurred at shorter wavelength (λ_{lasing}: 1.27~1.34 μm), corresponding to the QD excited state transition [15]. By contrast, it has remained more challenging to realize laser operations near the telecom C-band on Si substrates through the use of an MBL and conventional QW active region. Realizing a lattice constant close to that of InP by means of an MBL on Si substrate requires a more aggressive compositional grading. In addition, it is necessary to achieve sufficient suppression of both threading dislocations (TDs), originating from the larger lattice-mismatch, and formation of anti-phase domains. Nevertheless, QW active region lasers emitting near 1.55 μm, monolithically grown on Si substrates, have been demonstrated by either the use of a relatively thick (~13 μm) HVPE (hydride vapor phase epitaxy) grown InP buffer layer [8] on a miscut Si substrate or by using a pre-patterned (v-groove patterned) on-axis (001) Si substrates [9].

An understanding of the limiting factors for the device performance characteristics is lacking despite a number of demonstrations of lasing on either GaAs or Si substrate near the telecom C-band, have been reported to date, by employing an MBL. Here, we report on the use of InAs-based dislocation filters (DFs), either InAs quantum well (QW) DFs on nominally exact (001) GaAs substrate or InAs quantum dot (QD) DFs on on-axis (100) Si, *without pre-patterning*, which result in a high quality InP MBL formed by metal-organic vapor phase epitaxy (MOVPE). Subsequent growth and device characterizations of complete laser structures employing $In_{0.65}Ga_{0.35}As$ 3-QW active regions grown on these types of MBL, as well as on (001) InP substrate, are presented in the systematic comparison manner. In addition, nanoscale analysis within the QW active region by transmission electron microscopic (TEM) investigation for these devices was performed and correlated to the observed device characteristics.

2. Experimental details

The complete device structure grown on InP MBL on GaAs substrate is schematically represented in Fig. 1. The crystal growth was carried out at 100 Torr within a vertical chamber MOVPE (3×2" multi-wafer) reactor with a close-coupled showerhead (CCS) gas delivery system using purified H_2 as a carrier gas.

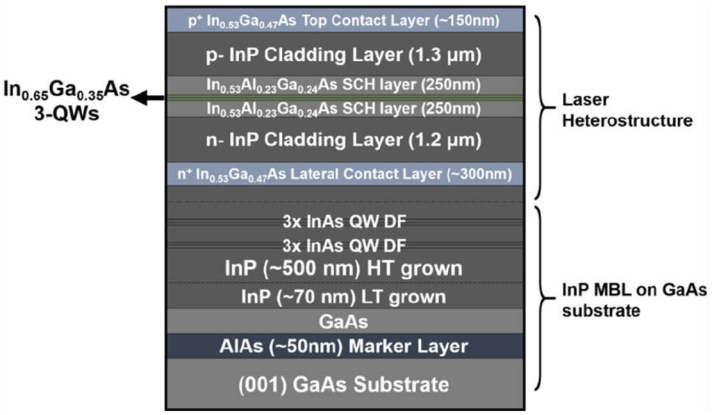

Fig. 1. Structure details of the complete laser structure grown on InP MBL on (001) GaAs substrate where InP MBL employs 2 period of triple layered InAs QW dislocation filters (DF).

Optics EXPRESS

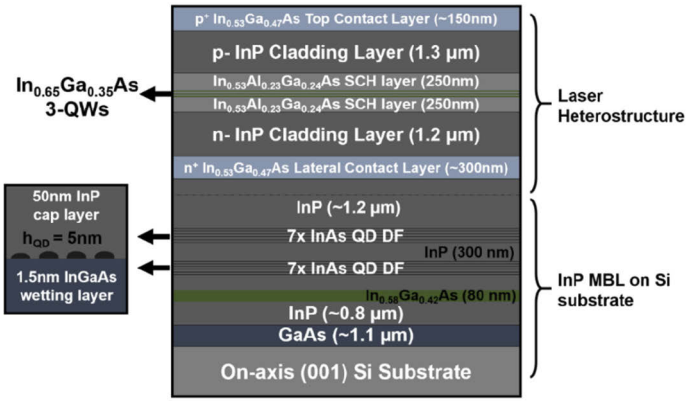

Fig. 2. Structure details of the complete laser structure grown on InP MBL on on-axis (001) Si substrate.

After 5 min of deoxidation and thermal cleaning under an AsH_3 overpressure, the growth on (100) GaAs substrate was initiated with 100nm-thick GaAs buffer layer, 50nm-thick AlAs marker layer, and 100nm-thick GaAs layer, subsequently, using trimethylgallium (TMGa), trimethylaluminum (TMAl), and arsine (AsH_3) as precursors. The temperature was then ramped down to 460°C, and a 70 nm-thick InP layer was grown by using trimethylindium (TMIn) and PH_3. After the growth of InP at 460°C, the temperature was ramped up to 625°C and a 500 nm-thick InP layer was grown. Then, the temperature was ramped down again to 475°C for the growth of 3-period InAs/InP (8/17nm) superlattice (SL) as a dislocation filter without growth interruptions. The growth temperature was then again raised to 625°C again and a 200 nm-thick InP layer was grown at V/III = 54. After the growth of additional 3-period InAs/InP (6/17nm) SLs at the lowered temperature of 475°C, a 300 nm-thick InP layer was finally grown on the InP MBL structure. These successive temperature ramping is believed to act as "thermal cycling", reducing the threading dislocation density (TDD), as reported for either GaAs or InP heteroepitaxy on Si [16,17]. The growth parameters used for the InP MBL on GaAs substrate are summarized in Table 1.

Table 1. The growth parameters used for the InP MBL on GaAs substrate

Material	V/III ratio	Group III partial pressure (mTorr)	Thickness (nm)	Temperature (°C)
GaAs buffer layer	80	10.3	100	685
AlAs marker	120	8.2	50	685
GaAs	80	10.3	100	685
LT-InP	338	2.1	70	460
HT-InP	54	9.9	500	625
3-period InAs/InP	338	2.1	3x (8 / 17)	475
HT-InP	54	9.9	200	625
3-period InAs/InP	338	2.1	3x (8 / 17)	475
HT-InP	54	9.9	300	625

After the growth of InP buffer layer on GaAs substrate, the full laser structures were grown by using TMIn, TMAl, TMGa, AsH_3, and PH_3 with Si_2H_6 and diethyl-zinc (DEZn) as n-doping and p-doping precursors with the growth parameters summarized in Table 2. The structure contained a 3-period $In_{0.65}Ga_{0.35}As$ / $In_{0.5}Al_{0.26}Ga_{0.24}As$ (7/14 nm) active region, $In_{0.53}Al_{0.23}Ga_{0.24}As$

Optics EXPRESS

separate confinement heterostructure (SCH), InP cladding layers, and $In_{0.53}Ga_{0.47}As$ contact layers.

Table 2. The growth parameters used for the complete laser structure

Material	V/III ratio	TMIn partial pressure (mTorr)	TMIn/III	Carrier Density (dopant, cm^{-3})	Temp. (°C)
Semi insulating-InP	54	9.9	1	Semi-insulating (Fe)	650
n^+ $In_{0.53}Ga_{0.47}As$	63	5.6	0.6446	1×10^{19} (Si)	650
n-InP	54	9.9	1	4×10^{17} (Si)	650 → 625
$In_{0.53}Al_{0.23}Ga_{0.24}As$ SCH	74	5.6	0.6441	undoped	625
3x $In_{0.65}Ga_{0.35}As$ QW active region	79	5.6	0.6912	undoped	625
$In_{0.53}Al_{0.23}Ga_{0.24}As$ SCH	74	5.6	0.6441	undoped	625
p-InP	54	9.9	1	2×10^{17} (Zn)	625
p^+ $In_{0.53}Ga_{0.47}As$	63	5.6	0.6441	1×10^{19} (Zn)	625

The same complete laser structure, shown in Fig. 2, was also grown on the InP buffer layer, which employs InAs QD DFs, on Si substrate [18,19]. It is noted that for the thorough comparison studies, the same laser structure was grown simultaneously on a semi-insulating InP substrate as a reference.

After the full laser structure growth, 25μm-wide ridge waveguide lasers with side-bottom contact were fabricated by a standard photolithographic and metal lift-off process, as shown in Fig. 3. Successive selective wet etching was carried out to form ridge waveguide by using H_3PO_4:H_2O_2:H_2O = 1:1:8 and H_3PO_4:HCl = 3:1 in volume ratio. A 200nm-thick SiN_x, deposited by plasma-enhanced chemical vapor deposition, was used for electrical passivation and isolation. The wafer was thinned to 150μm. E-beam evaporation of Ti/Pt/Au (30/50/300nm) was used to form a metal electrode on p^+ $In_{0.53}Ga0_{.47}As$, while AuGe/Ni/Au (100/35/200nm) contact metallurgy was used for n^+ $In_{0.53}Ga0_{.47}As$. The contact metals were alloyed at 375°C for 30 sec using RTA. Devices were measured *as-cleaved* (*i.e.* no facet coatings) at room temperature under pulsed current operation with a cavity length of 2 mm.

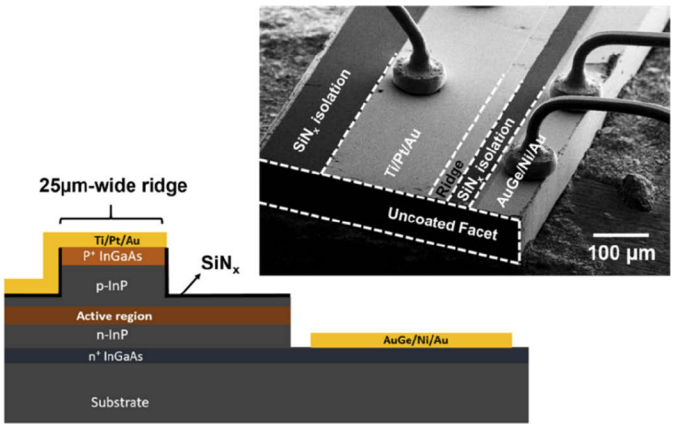

Fig. 3. Schematic view of cross section and top-view SEM of fabricated device structure

Lasing spectrum was measured using an optical spectrum analyzer while the output power from one facet was measured using a calibrated InGaAs photodiode in conjunction with an integrating sphere. In addition, the temperature sensitivity of the threshold current density and slope

Optics EXPRESS

efficiency were measured within the temperature range from 283 to 323K. Furthermore, scanning transmission electron microscopy (STEM) was used to investigate the threading dislocation (TD) within the device structure. TEM specimens were prepared by a focused ion beam (FIB) lift-out technique. Final thinning was performed with Ga^+ ions at 2 kV to minimize the surface damage associated with FIB sample preparation.

3. Results and discussions

Shown in Fig. 4. are the *in-situ* reflectance recorded during the growth of InP MBL on GaAs substrate and an atomic force microscopic (AFM) image taken before the growth of the complete laser device structure.

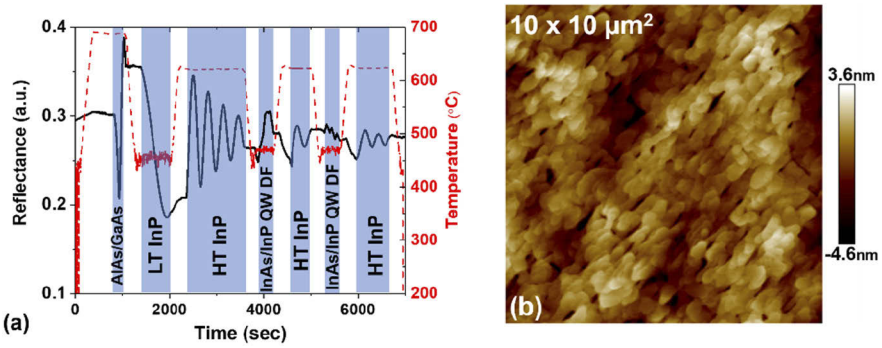

Fig. 4. (a) in situ reflectance during the growth of InP buffer layer on GaAs substrate and (b) Atomic force microscopic image taken before laser structure grown on InP MBL on GaAs substrate (RMS roughness: 1.04nm)

No apparent reduction in overall *in-situ* reflectance intensity was observed during the growth of InP MBL on GaAs substrate. Before the laser device structure growth, the root-mean-square (RMS) roughness was ~1.04 nm from the $10 \times 10\,\mu m^2$ AFM image. This RMS roughness value is significantly lower than the reported RMS roughness (~5nm) from a metamorphic InP layer grown on GaAs substrate, which also employs low-temperature InP nucleation layer [20]. We attribute this lower RMS roughness, presented in our study, to the use of InAs QW DF in conjunction with a series of temperature ramping, which is believed to act as "thermal cycling", reducing TDD, as reported for GaAs heteroepitaxy on Si substrate [17].

STEM bright field image for the complete laser structure grown on InP MBL on GaAs substrate is shown in Fig. 5, which was used to quantify the effects of InAs QW DF on TDD.

While it is not feasible to obtain an accurate measurement of threading dislocation density (TDD) from this cross-sectional view, a significant reduction in the TD count within the presented limited field of view was observed as a result of the use of InAs QWs as a dislocation filter. This observation agrees well with a reported observation from GaAs/Si heteroepitaxy where a strained superlattice was used a dislocation filter [21]. A larger field of view STEM images or in-plane images are needed to more accurately quantify the TDD.

The RMS roughness of the InP buffer layer grown on the on-axis (001) Si substrate was measured to be 5.4 nm with the TDD of $\sim 3 \times 10^8 cm^2$ as reported elsewhere from the identical InP MBL sample [22], which is significantly higher than the RMS roughness obtained from the InP buffer layer on the GaAs substrate, most likely due to a higher TDD and a higher stacking fault density, originating from a larger lattice mismatch between InP and Si.

As shown in Fig. 6(a), the laser structures grown on InP MBL on mismatched substrates exhibit well-defined superlattice fringes, which are identical to those of structure grown on InP substrate, yielding identical average composition and thickness of QW and barrier within the active region.

Optics EXPRESS

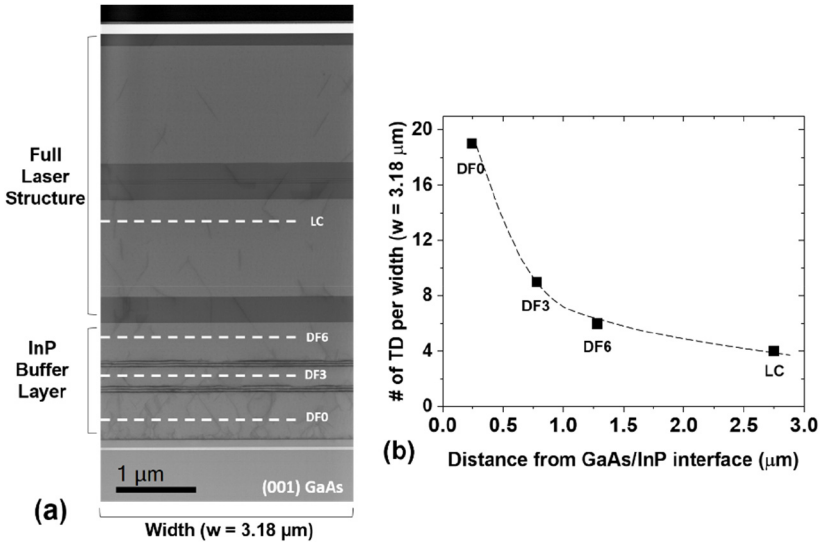

Fig. 5. (a) STEM bright field image within a limited field of view where dislocations appear as dark lines (b) the number of threading dislocation (# of TD) per width (w = 3.18μm) counted from the STEM image shown in Fig. 5(a)

The full-width-half-max (FWHM) of (004) InP peak, which is often used to evaluate the defect density of the material grown on mismatched substrate [23]. The device structure grown on InP MBL on GaAs substrate possessed a FWHM of 216 arcsec, while the observed FWHM from the device structure on InP MBL on Si substrate was 320 arcsec. Both values are significantly higher than that from the structure grown on InP substrate (72 arcsec). The observed broader FWHM in HRXRD scan from the laser structure on either GaAs or Si substrate can possibly be ascribed to a higher TDD [24]. A reduced contrast in Pendellösung fringes was observed as the lattice-mismatch increased in comparison to that of the device structure grown on InP, as shown in Fig. 6(b), which can be indicative of less abrupt interfaces within the 3-QW active region.

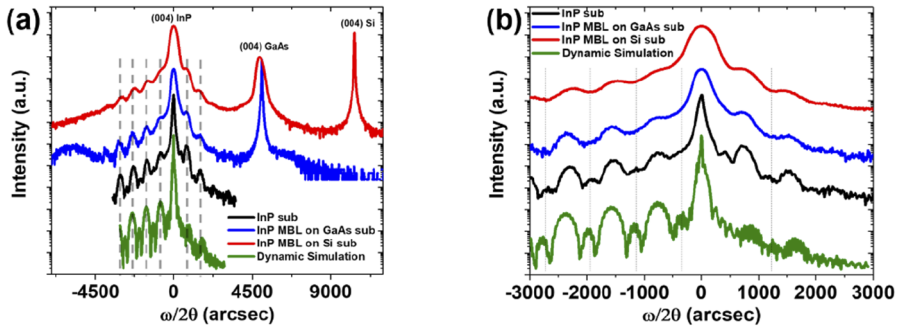

Fig. 6. (a) High resolution X-ray diffraction (HRXRD) $\omega/2\theta$ scans around (004) reflection from the laser structure grown on InP substrate and InP MBLs on either Si or GaAs substrate and (b) magnified view around (004) InP peak.

Shown in Fig. 7 is the output power – injection current relation (PI) under pulsed operation at 20°C from the devices grown on either InP substrate or InP MBLs on Si or GaAs substrate. The threshold current densities (J_{th}) of the device grown on either GaAs or Si substrate were 0.96 and 1.6 kA/cm^2, respectively, while that of the device grown on InP substrate was 0.6

Optics EXPRESS

kA/cm^2. The higher J_{th} can be due to a higher density of non-radiative recombination centers, presumably from a higher TDD. Nevertheless, the obtained J_{th} values are relatively low for the 3-QW active region, in comparison to prior reports as summarized in Table 3. It must be noted that a significantly smaller slope efficiency was obtained from the device grown on Si substrate (η_{slope} = 26.5mW/A), while those from the devices on either InP substrate or GaAs substrate were η_{slope} = 174mW/A and η_{slope} = 130mW/A, respectively. This observation can be indicative of a higher internal optical loss within the laser cavity, as a results of a higher defect density [25] and/or a significantly lower injection efficiency above the threshold, which can be greatly affected by the carrier leakage rate [26]. The carrier leakage rate can be, then, sensitive to the operation temperature, due to the nature of thermionic process.

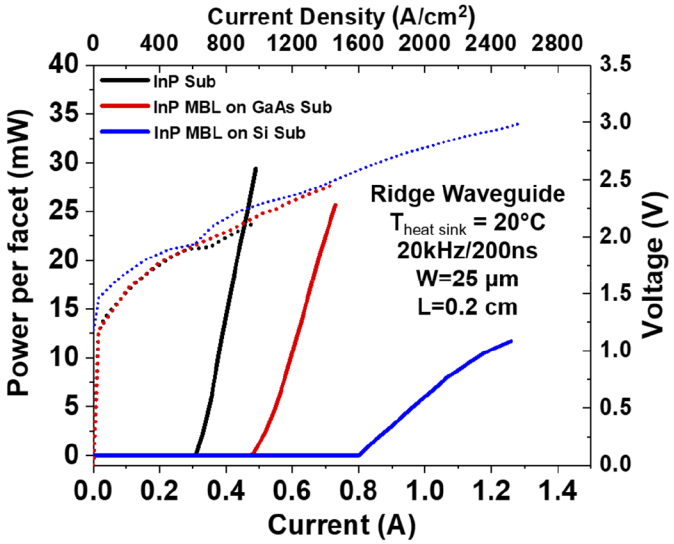

Fig. 7. The output power – injection current relation of the laser devices grown on InP substrate and InP MBLs on either GaAs or Si substrates tested at 20°.

Table 3. Summary of prior reports on the QW laser diodes grown on mismatched substrate emitting near telecom C-band

Substrate	(Crystal Growth Method) Structure	λ_{lasing}	J_{th}
GaAs	**(MBE)** $In_{0.6}Ga_{0.4}As$ **SQW** on $In_{0.32}Ga_{0.68}As$ MBL[11]	1.58 μm	0.49kA/cm^2
GaAs	**(MBE)** GaSb/AlGaSb **6-QWs** by IMF[12]	1.65 μm	3kA/cm^2
Si	**(HVPE + MOVPE)** InGaAs **6-QWs** on HVPE-InP buffer layer[8]	1.54 μm	3kA/cm^2(CW)
Si	**(MOVPE)** InGaAs **7-QWs** on InP buffer layer on **V-grooved on-axis Si**[9]	1.5 μm	3.3kA/cm^2

The temperature sensitivities of the threshold current (I_{th}), $T_0 = (d \ln I_{th}/dT)^{-1}$ and slope efficiency $T_1 = -(d \ln \eta_{slope}/dT)^{-1}$, from those grown on either InP, GaAs, or Si substrate are summarized in Fig. 8(a) and 8(b). A lower T_0 (41K) was observed from the device grown on Si substrate while the devices grown on either GaAs substrate or InP substrate exhibited similar T_0 values (51~52K). Significantly lower T_1 values (113K and 53K from 10 to 35°C) were obtained from those grown on either GaAs or Si substrate, compared to that (150K) from the device on InP substrate. Lower T_1 values can imply a significant carrier leakage out of the QW active region, as investigated by a prior study [26]. It is noted that the T_0 values, obtained here, are generally small due to inherently weak carrier confinement at the interface between AlInGaAs SCH and InP cladding layer as well as that of AlInGaAs SCH and InGaAs QW [27–28] and due to Auger

Optics EXPRESS

recombination [29]. Therefore, together with optimization in the heterostructure, T_0 and T_1 can be somewhat improved [30].

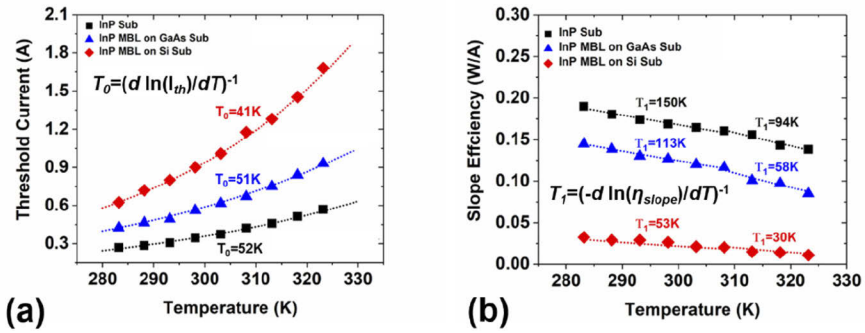

Fig. 8. (a) The change in the threshold current as a function of heat-sink temperature from 10 to 50°C (b) The change in the slope efficiency as a function of heat-sink temperature from 10 to 35°C and from 35 to 50°C, respectively.

In addition, a significant blue shift in the lasing wavelength was observed from the device grown on Si substrate (λ_{lasing} = 1623 nm), while the devices grown on either InP or GaAs substrates exhibit similar lasing wavelength (λ_{lasing} = 1652 ~ 1654 nm), as shown in Fig. 9. The observed blue-shift may stem from a different potential profile of the QW active region on the Si substrate, carrier band-filling due to the higher threshold current density, and/or the potentially higher internal optical loss by a higher defect density [25].

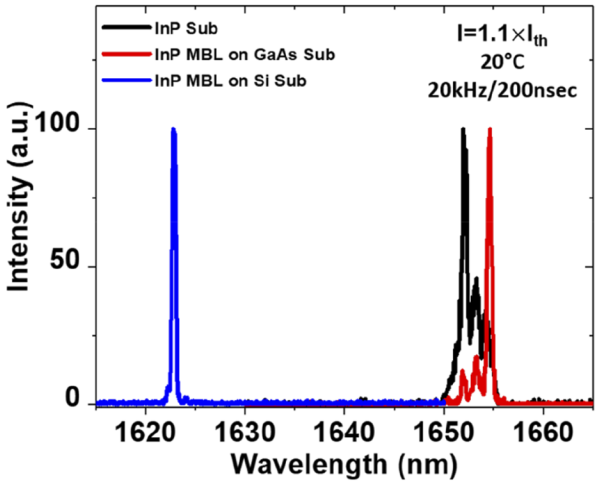

Fig. 9. Lasing spectrum above lasing threshold of the laser devices grown on either InP substrate or InP MBLs on GaAs or Si substrates tested at 20°C.

STEM investigation revealed a graded interface of the $In_{0.65}Ga_{0.35}As$ QW within the active region grown on Si substrate in comparison to that grown on InP substrate as shown in Fig. 10. This observation is consistent with the HRXRD $\omega/2\theta$ scan, shown in Fig. 6(b) where a less sharp contrast in Pendellösung fringes was observed. It must be noted that while the profile in Fig. 10(c) appears as a compositionally graded interface, it can possibly reflect a rough interface, which was evidenced by the AFM RMS roughness (5.4 nm) and the thin nature of the STEM sample. Other techniques, such as atom probe tomography, are necessary to quantify the actual compositional

Optics EXPRESS

grading, which is the subject of an ongoing investigation. Nevertheless, prior studies have shown that either graded interface or rougher interface can lead to a significant carrier leakage [31–32], and is consistent with the observed low slope efficiency (26.5mW/A) and low T_1 (53K) from the device grown on Si substrate. Prior studies have shown that a subsequent post-growth thermal annealing of a QW active region laser can lead to a similar interfacial compositional grading, to that observed in Fig. 10, as well as a blue shift in the emission wavelength similar to that from the device grown on Si substrate [32].

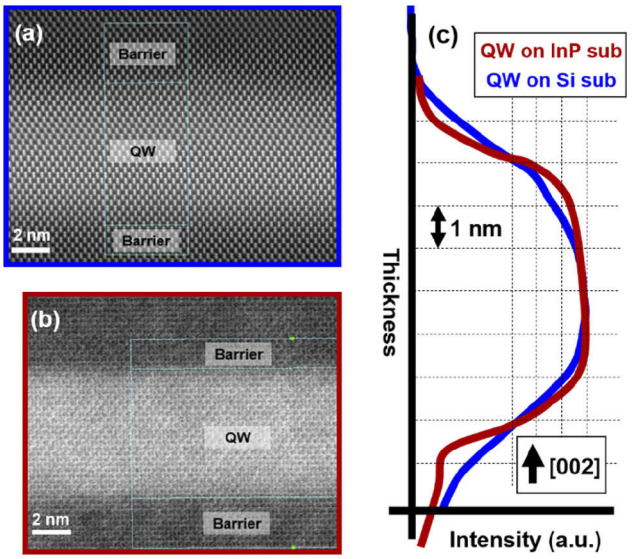

Fig. 10. (a) STEM dark field image of an $In_{0.65}Ga_{0.35}As$ QW within the active region grown on Si substrate, (b) STEM dark field image of an $In_{0.65}Ga_{0.35}As$ QW within the active region grown on InP substrate, and (c) corresponding STEM intensity profile showing a more graded/rougher interface of the $In_{0.65}Ga_{0.35}As$ QW on Si substrate.

Figure 11 reveals a V-pit within the active region grown on Si substrate, which was apparently nucleated from a TD. In a prior study, the formation of similar V-pits was ascribed due to a local variation in the growth rate when two twinned planes kink and annihilate [33]. Further investigation on the formation of this V-pit and extracting its volumetric density remains as a future work. It is noteworthy that the presence of V-pits can possibly lead to the optical scattering within the laser cavity, increasing the internal optical loss, which, in turn, can result in a lower slope efficiency Performing internal parameter extraction techniques such as cavity length analysis [34] or segmented contact method [35], combined with additional larger area TEM imaging, will be necessary to experimentally identify the impact of these V-pits on the device performance.

Optics EXPRESS

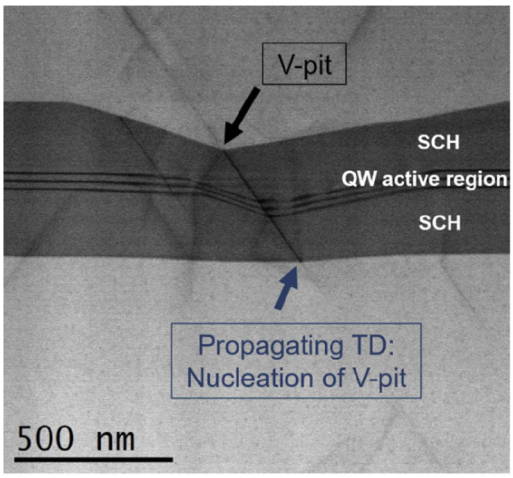

Fig. 11. STEM image showing a V-pit, which is apparently nucleated by a threading dislocation.

4. Conclusion

In conclusion, we have carried out a systematic comparison study on the 3-QW $In_{0.65}Ga_{0.35}As$ active region diode lasers grown on mismatched substrates (GaAs and Si) by MOVPE. High performance devices, emitting near the telecom C-band, were demonstrated by employing an InP MBL with InAs nanostructure-based dislocation filters on either GaAs or Si substrate with relatively low J_{th} values (0.96 and 1.6 kA/cm^2, respectively). While the observed T_0 value (51K) from the device grown on InP MBL on GaAs substrate was similar to the value (52 K) obtained from the device grown on InP substrate, the devices grown on Si substrate exhibited a significantly lower slope efficiency (~26.5 mW/A) and characteristic temperatures, T_0~41K and T_1~53K, together with a blueshift in the lasing wavelength. The STEM investigation revealed compositionally graded and / or rougher interfaces of $In_{0.65}Ga_{0.35}As$ QW active region grown on Si substrate, which was correlated to the presence of severe active region carrier leakage evident from the observed device characteristics. This observation by STEM and device characterization both suggest that further reduction in TDD as well as improvement in the interfacial abruptness are necessary to further improve the performance of the QW-based lasers grown on mismatched substrate. In addition, the presence of V-pits within the active region on Si substrate could contribute to a higher internal optical loss, leading to the lower observed laser slope efficiency.

Funding

Division of Materials Research (1121288); Division of Electrical, Communications and Cyber Systems (1806285); Army Research Office (W911NF-16-1-0298); Research Grants Council, University Grants Committee (16245216); Innovation and Technology Fund (ITS/273/16FP); The Aerospace Corporation's Sustained Experimentation and Research for Program Applications (SERPA).

Acknowledgments

Honghyuk Kim appreciates the travel grant awards from the Graduate School, and from the department of Electrical and Computer Engineering at the University of Wisconsin-Madison.

Optics EXPRESS

Disclosures

The authors declare that there are no conflicts of interest related to this article

References

1. M. Zaknoune, B. Bonte, C. Gaquiere, Y. Cordier, Y. Druelle, D. Theron, and Y. Crosnier, "InAlAs/InGaAs metamorphic HEMT with high current density and high breakdown voltage," IEEE Electron Device Lett. **19**(9), 345–347 (1998).
2. W. T. Tsang, "Chemical beam epitaxy of InP and GaAs," Appl. Phys. Lett. **45**(11), 1234–1236 (1984).
3. Z. Griffith, Y. Kim, M. Dahlström, A. C. Gossard, and M. J. W. Rodwell, "InGaAs-InP metamorphic DHBTs grown on GaAs with lattice-matched device performance and f_τ, $f_{max} > 268$ GHz," IEEE Electron Device Lett. **25**(10), 675–677 (2004).
4. B. Shi, S. Zhu, Q. Li, C. W. Tang, Y. Wan, E. L. Hu, and K. M. Lau, "1.55 μm room-temperature lasing from subwavelength quantum-dot microdisks directly grown on (001) Si," Appl. Phys. Lett. **110**(12), 121109 (2017).
5. D. Liang, D. C. Chapman, Y. Li, D. C. Oakley, T. Napoleone, P. W. Juodawlkis, C. Brubaker, C. Mann, H. Bar, O. Raday, and J. E. Bowers, "Uniformity study of wafer-scale InP-to-silicon hybrid integration," Appl. Phys. A **103**(1), 213–218 (2011).
6. R. Go, H. Krysiak, M. Fetters, P. Figueiredo, M. Suttinger, J. Leshin, X. M. Fang, J. M. Fastenau, D. Lubyshev, A. W. K. Liu, A. Eisenbach, M. J. Furlong, and A. Lyakh, "Room temperature operation of quantum cascade lasers monolithically integrated onto a lattice-mismatched substrate," Appl. Phys. Lett. **112**(3), 031103 (2018).
7. M. Razeghi, M. Defour, R. Blondeau, F. Omnes, P. Maurel, and O. Acher, "First cw operation of a $Ga_{0.25}In_{0.75}As_{0.5}P_{0.5}$-InP laser on a silicon substrate," Appl. Phys. Lett. **53**(24), 2389–2390 (1988).
8. M. Sugo, H. Mori, Y. Sakai, and Y. Itoh, "Stable cw operation at room temperature of a 1.5-μm wavelength multiple quantum well laser on a Si substrate," Appl. Phys. Lett. **60**(4), 472–473 (1992).
9. S. Zhu, B. Shi, Q. Li, and K. M. Lau, "Room-temperature electrically-pumped 1.5 μm InGaAs/InAlGaAs laser monolithically grown on on-axis (001) Si," Opt. Express **26**(11), 14514–14523 (2018).
10. M. Tachikawa and H. Mori, "Dislocation generation of GaAs on Si in the cooling stage," Appl. Phys. Lett. **56**(22), 2225–2227 (1990).
11. M. Yamaguchi and C. Amano, "Efficiency calculations of thin-film GaAs solar cells on Si substrates," J. Appl. Phys. **58**(9), 3601–3606 (1985).
12. I. Tångring, H. Q. Ni, B. P. Wu, D. H. Wu, Y. H. Xiong, S. S. Huang, Z. C. Niu, S. M. Wang, Z. H. Lai, and A. Larsson, "1.58 μm InGaAs quantum well laser on GaAs," Appl. Phys. Lett. **91**(22), 221101 (2007).
13. M. Mehta, A. Jallipalli, J. Tatebayashi, M. N. Kutty, A. Albrecht, G. Balakrishnan, L. R. Dawson, and D. L. Huffaker, "Room-Temperature Operation of Buffer-Free GaSb–AlGaSb Quantum-Well Diode Lasers Grown on a GaAs Platform Emitting at 1.65 μm," IEEE Photonics Technol. Lett. **19**(20), 1628–1630 (2007).
14. H. Y. Liu, Y. Qiu, C. Y. Jin, T. Walther, and A. G. Cullis, "1.55 μm InAs quantum dots grown on a GaAs substrate using a GaAsSb metamorphic buffer layer," Appl. Phys. Lett. **92**(11), 111906 (2008).
15. Y. C. Xin, L. G. Vaughn, L. R. Dawson, A. Stintz, Y. Lin, L. F. Lester, and D. L. Huffaker, "InAs quantum-dot GaAs-based lasers grown on AlGaAsSb metamorphic buffers," J. Appl. Phys. **94**(3), 2133–2135 (2003).
16. S. Zhu, B. Shi, Q. Li, and K. M. Lau, "1.5 μm quantum-dot diode lasers directly grown on CMOS-standard (001) silicon," Appl. Phys. Lett. **113**(22), 221103 (2018).
17. M. Yamaguchi, A. Yamamoto, M. Tachikawa, Y. Itoh, and M. Sugo, "Defect reduction effects in GaAs on Si substrates by thermal annealing," Appl. Phys. Lett. **53**(23), 2293–2295 (1988).
18. B. Shi, Q. Li, and K. M. Lau, "Self-organized InAs/InAlGaAs quantum dots as dislocation filters for InP films on (001) Si," J. Cryst. Growth **464**, 28–32 (2017).
19. B. Shi, Q. Li, and K. M. Lau, "Epitaxial growth of high quality InP on Si substrates: The role of InAs/InP quantum dots as effective dislocation filters," J. Appl. Phys. **123**(19), 193104 (2018).
20. W. Zhou, C. W. Tang, J. Zhu, K. M. Lau, Y. Zeng, H. G. Liu, N. G. Tao, and C. R. Bolognesi, "Metamorphic Heterostructure InP/GaAsSb/InP HBTs on GaAs Substrates by MOCVD," IEEE Electron Device Lett. **28**(7), 539–542 (2007).
21. I. George, F. Becagli, H. Y. Liu, J. Wu, M. Tang, and R. Beanland, "Dislocation filters in GaAs on Si," Semicond. Sci. Technol. **30**(11), 114004 (2015).
22. A. Rajeev, B. Shi, Q. Li, J. D. Kirch, M. Cheng, A. Tan, H. Kim, K. Oresick, C. Sigler, K. M. Lau, T. F. Kuech, and L. J. Mawst, "III–V Superlattices on InP/Si Metamorphic Buffer Layers for $\lambda \approx 4.8$ μm Quantum Cascade Lasers," Phys. Status Solidi A **216**(1), 1800493 (2018).
23. H. Amano, N. Sawaki, I. Akasaki, and Y. Toyoda, "Metalorganic vapor phase epitaxial growth of a high quality GaN film using an AlN buffer layer," Appl. Phys. Lett. **48**(5), 353–355 (1986).
24. V. M. Kaganer, R. Köhler, M. Schmidbauer, R. Opitz, and B. Jenichen, "X-ray diffraction peaks due to misfit dislocations in heteroepitaxial structures," Phys. Rev. B **55**(3), 1793–1810 (1997).
25. S. Shutts, C. P. Allford, C. Spinnler, Z. Li, A. Sobiesierski, M. Tang, H. Liu, and P. M. Smowton, "Degradation of III–V Quantum Dot Lasers Grown Directly on Silicon Substrates," IEEE J. Sel. Top. Quantum Electron. **25**(6), 1–6 (2019).

Optics EXPRESS

26. N. Tansu, J. Yeh, and L. J. Mawst, "Experimental evidence of carrier leakage in InGaAsN quantum-well lasers," Appl. Phys. Lett. **83**(11), 2112–2114 (2003).
27. N. Ohnoki, G. Okazaki, F. Koyama, and K. Iga, "Record high characteristic temperature (T_0 = 122 K) of 1.55 μm strain-compensated AlGaInAs/AlGaInAs MQW lasers with AlAs/AlInAs multiquantum barrier," Electron. Lett. **35**(1), 51–52 (1999).
28. J. Piprek, J. K. White, and A. J. SpringThorpe, "What limits the maximum output power of long-wavelength AlGaInAs/InP laser diodes?" IEEE J. Quantum Electron. **38**(9), 1253–1259 (2002).
29. E. P. O'Reilly and M. Silver, "Temperature sensitivity and high temperature operation of long wavelength semiconductor lasers," Appl. Phys. Lett. **63**(24), 3318–3320 (1993).
30. T. Garrod, D. Olson, M. Klaus, C. Zenner, C. Galstad, L. Mawst, and D. Botez, "50% continuous-wave wallplug efficiency from 1.53 μm-emitting broad-area diode lasers," Appl. Phys. Lett. **105**(7), 071101 (2014).
31. A. Bhattacharya, L. J. Mawst, S. Nayak, J. Li, and T. F. Kuech, "Interface structures of InGaAs/InGaAsP/InGaP quantum well laser diodes grown by metalorganic chemical vapor deposition on GaAs substrates," Appl. Phys. Lett. **68**(16), 2240–2242 (1996).
32. G. Zhang, J. Näppi, A. Ovtchinnikov, H. Asonen, and M. Pessa, "Effects of rapid thermal annealing on lasing properties of InGaAs/GaAs/GaInP quantum well lasers," J. Appl. Phys. **72**(8), 3788–3791 (1992).
33. T. Orzali, A. Vert, B. O'Brien, J. L. Herman, S. Vivekanand, R. J. W. Hill, Z. Karim, and S. S. Papa Rao, "GaAs on Si epitaxy by aspect ratio trapping: Analysis and reduction of defects propagating along the trench direction," J. Appl. Phys. **118**(10), 105307 (2015).
34. L. A. Coldren, S. W. Corzine, and M. L. Mashanovitch, *Diode lasers and photonic integrated circuits* (John Wiley & Sons, 2012)
35. P. Blood, G. M. Lewis, P. M. Smowton, H. Summers, J. Thomson, and J. Lutti, "Characterization of semiconductor laser gain media by the segmented contact method," IEEE J. Sel. Top. Quantum Electron. **9**(5), 1275–1282 (2003).